ChemPubSoc Europe

DOI: 10.1002/chem.201500230

CHEMISTRY
A European Journal
Full Paper

Sensitizers

Stable and Easily Accessible Functional Dyes: Dihydrotetraazaanthracenes as Versatile Precursors for Higher Acenes

Dominique Mario Gampe,[a] Martin Kaufmann,[a, b] Dörthe Jakobi,[a] Torsten Sachse,[b] Martin Presselt,[b] Rainer Beckert,*[a] and Helmar Görls[c]

Abstract: A series of new dihydrotetraazaanthracenes and one new dihydrotetraazatetracene as substances for applications in organoelectronic devices and as suitable building blocks for higher azaacenes was synthesised. The condensation of aromatic diamines with dichlorodicyanopyrazine led to these tricyclic/tetracyclic compounds. Syntheses of *N*-substituted phenylenediamines were developed to enable the introduction of multiple functional groups such as ester, amino, or nitro groups on the chromophoric system. Relationships between the structure and the spectroscopic properties could be derived from UV/Vis absorption and fluorescence spectroscopy, as well as by DFT and TD-DFT calculations of molecular and aggregate structures. The absorption spectra are dominated by π–π^* transitions of the single molecules, whereas aggregation needs to be taken into account to obtain reasonable agreement between theory and experiment in certain cases. Single-crystal X-ray analyses were carried out to examine the morphology and solid packing effects. Finally, a dihydrotetraazaanthracene was used as a building-block to create a mesoionic octaazapentacene.

Introduction

Significant progress is being made in the development of organic electronic and optoelectronic devices.[1] However, many of the recently developed material systems contain scarce or expensive materials, such as redox systems containing ruthenium or fullerenes as acceptor materials, respectively.[2] Generally, the use of expensive materials can negate the advantage of inexpensive, large-scale production of organic electronic devices.[3] Hence, there is huge demand for replacing such systems with stable organic dyes, for example, in solar cells.[4] Since the successful stabilisation of pentacene, linear-condensed acenes have found many applications as versatile organic semiconductors.[5] The replacement of CH by other atoms (mainly N or S) results in heteroacenes in which a different reactivity can be observed. The introduction of nitrogen atoms, particularly, leads to novel properties such as reduced HOMO-LUMO gaps, and especially to dramatically increased chemical stabilities.[6] Recent reviews[7] show that aza-substituted acenes are emerging in charge transport materials as well as in other functional materials. Among the azaacenes, linear systems, for example, **1** "Pyrazinacenes",[8] comprise by far the majority of derivatives. However, the synthesis of higher azaacenes remains challenging because of 1) limited access to appropriate diamines and the corresponding bis-electrophilic partners, 2) low yields of reactions with bis-electrophiles (classic conditions, partially Pd-catalysed), and 3) poor solubility of the azaacenes because of severe aggregation phenomena, which complicates characterisation and processing.

Most of the syntheses described use the condensation reaction of *vicinal* diamines **1** with partners **2** possessing vicinal leaving groups X, as depicted in Scheme 1, in which X = OH,[9] X = halogen: nucleophilic heteroaromatic substitution[10] or Pd-catalysis,[10c] X = CN,[11] diketones,[12] and quinone imines.[13] In all of these cases, the rings A and B themselves can be hetero-

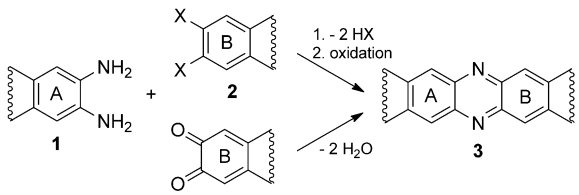

Scheme 1. Retrosynthetic approach to azaacenes.

[a] *Dipl.-Chem. D. M. Gampe, Dipl.-Chem. M. Kaufmann, D. Jakobi, Prof. Dr. R. Beckert*
Friedrich Schiller University Jena
Institute of Organic and Macromolecular Chemistry
Humboldtstraße 10, 07743 Jena (Germany)
E-mail: rainer.beckert@uni-jena.de

[b] *Dipl.-Chem. M. Kaufmann, M. Sc. T. Sachse, Dr. M. Presselt*
Friedrich Schiller University Jena
Institute of Physical Chemistry
Helmholtzweg 4, 07743 Jena (Germany)

[c] *Dr. H. Görls*
Friedrich Schiller University Jena
Institute of Inorganic and Analytical Chemistry
Humboldtstraße 8, 07743 Jena (Germany)

Supporting information for this article is available on the WWW under http://dx.doi.org/10.1002/chem.201500230.

cycles and members of bi- and polycyclic compounds. Cycloadditions of quinodimethides generated in situ[6d,7d] and oxidative *ortho*-annulations,[14a] as well as special methods, for example, for hexaazaanthracenes[14b] and hexaazaacridines,[14c] are rather exceptional.

Tetraazaanthracenes were synthesised in 1988 by the condensation of phenylenediamines with 5,6-dichloro-2,3-dicyanopyrazine;[15] however, their first use as strong acceptors in the form of n-type FET devices was reported in 2004.[16] Miao and co-workers took advantage of these compounds as building blocks for the production of highly electron-deficient hexaazapentacenes and their dihydro precursors.[17]

In the present work, we focus on the synthesis and characterisation of new derivatives of dihydrotetraazaanthracenes **16** and **17** (Scheme 2), because they are easily accessible, starting from a functionalised diamine **10** and **12**, and 5,6-dichloro-2,3-dicyanopyrazine (**14**). We were particularly interested in the introduction of functional substructures R into diamines that are able to preserve the corresponding dihydroanthracene forms. The substitution at the amino group causes a "frozen" dihydro form and, consequently, prevents oxidation by air. There are examples that such dihydro derivatives show much higher stabilities[18] and intense fluorescence[7c,10a] compared with the fully aromatic species. The simple introduction of substituents enabled us to synthesise a multitude of different dihydroazaanthracenes. The reactions tolerate nearly all functionalities. Therefore, it is possible to introduce electron-withdrawing and electron-donating moieties and, furthermore, solubility-improving groups. Halogen atoms for further cross-coupling experiments and alkyl chains possessing ester groups as precursors for amphiphilic features can also be obtained. The nitro-substituted dihydrotetraazaanthracenes **17** are expected to allow access to higher azaacenes by reduction and subsequent condensation reactions, whereas compounds **16** offer the possibility of modifications to the ester group. In addition, they might serve as precursors for hexaazapentacenes by nucleophilic substitution of the cyano groups.[8,17] To study the properties of extended π-systems, derivative **15** and angular tetracene **18** were both integrated into the study. To investigate the interactions between substituents and dihydroazaacene chromophores, UV/Vis absorption and emission spectroscopy measurements were performed, both of which were supplemented by quantum chemical simulations of the spectral features and line-fit analyses of the experimental spectra.

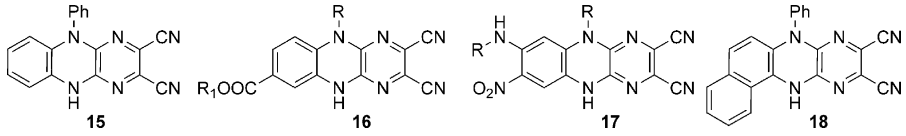

Scheme 2. Synthesised tetraaza-substituted dihydroanthracenes.

Results and Discussion

Syntheses

Diamines **10** can be obtained in four steps, starting with 4-fluoro benzoic acid through nitration,[19a] followed by esterification,[19b] nucleophilic fluoride substitution and reduction (Scheme 3).[20] The vicinal diamines **12** were prepared starting with 1,5-dichloro-2,4-dinitrobenzene by aminolyses to give **8**.[21] Generally, the reduction of both nitro groups in **9** is possible; however, the tetramino derivatives of type **11** proved to be very sensitive to oxidation and tended to decompose rapidly. Naphthalene derivative **13** was synthesised by azo coupling of commercially available 2-phenylamino-naphthalene with diazotated aniline and subsequent reduction with sodium dithionite.[22]

The model substance **15** was synthesised by cyclisation of *N*-phenyl-*o*-phenylenediamine and **14** (Scheme 4). Triamines **12**, diamines **10**, and naphthalene derivative **13** were cyclised with **14** under the exclusion of oxygen. In all cases, dihydrotetraazaanthracenes **16** and **17** and the angularly fused dihydrotetraazatetracene **18** were isolated as the main products.

Nitro-substituted derivatives **17** and the tetracene **18** show an intense red colour in both the solid state and in solution, whereas derivatives of type **16** were obtained as orange crystals. All derivatives were fully characterised by means of elemental analysis (EA), MS and NMR experiments.

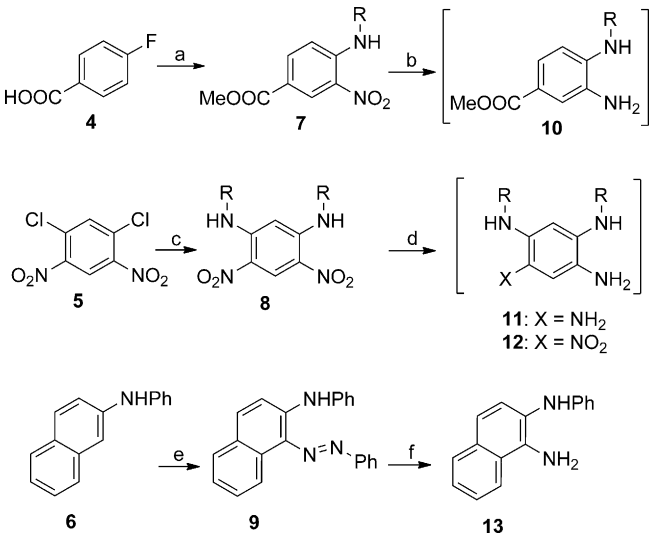

Scheme 3. Syntheses of vicinal diamines. Reagents and conditions: a) 1. KNO_3, H_2SO_4;[19a] 2. $SOCl_2$, MeOH;[19b] 3. R-NH_2: 36–99%; b) H_2,Pd/C, EtOH; c) EtOH, R-NH_2: 40–97%; d) Raney-Nickel, 30% NH_2NH_2, EtOH; e) Ph-NH_2, $NaNO_2$, EtOH/H_2O;[22a] f) NaS_2O_4, DMF.[22b]

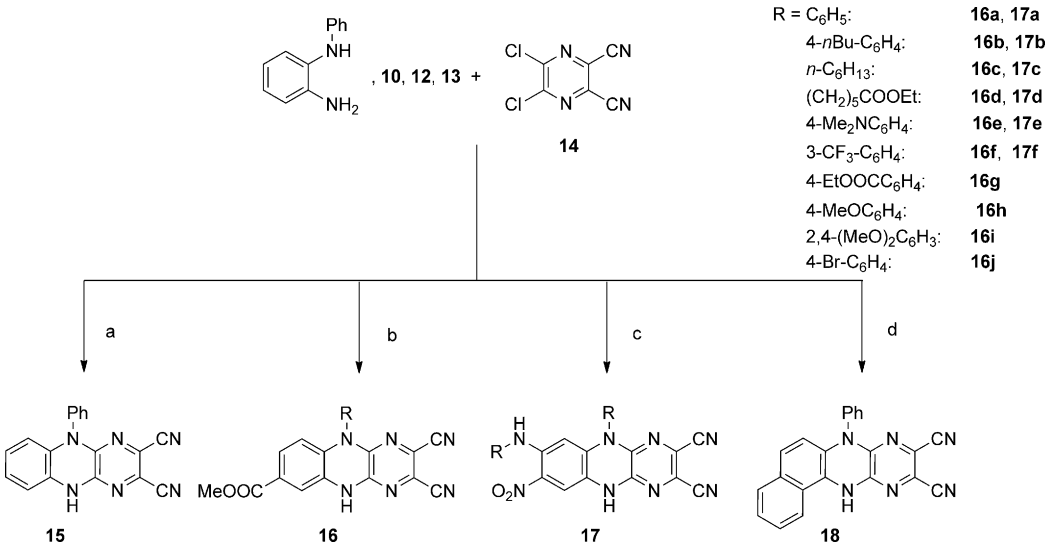

Scheme 4. Syntheses of dihydrotetraazaanthracenes **15**–**17** and dihydrotetraazatetracene **18**. Reagents and conditions: a) dioxane, 30 min reflux, 97%; b) EtOH, reflux, 18–65%; c) dioxane, 4 h reflux, overnight 80 °C, 18–35%; d) dioxane, DIPEA, 4 h reflux, 68%.

Dihydrotetraazaanthracenes 16

Single crystals of **16h** and **16d** that were suitable for X-ray crystallographic analysis were grown by evaporating the solvent from solutions in acetonitrile (**16h**) or acetone (**16d**). The resulting crystal structures are illustrated in Figure 1. The 4-methoxyphenyl substructure in derivative **16h** is distorted with an angle of 78.09° (C4-N2-C11-C12) out of plane. The bond lengths C4–N2, N2–C3, C9–N3, and N3–C10 indicate the involvement of the lone pair of N2 and N3 in the conjugated system.

Contrary to expectations, π–π interactions of the neighbouring stacks of **16h** cannot be observed. As depicted in Figure 2, two molecules form a point symmetric dimer through H-bridges that connect to the next dimer due to the π–π interactions of the 4-methoxyphenyl groups, thus generating a chain-like supramolecule. Despite having a similar structure, derivative **16d** coordinates a solvent molecule at the cyclic NH group, which efficiently prevents the formation of dimers and allows the formation of the π–π-stacking framework.

All derivates of type **16** show a similar UV/Vis absorption behaviour. Typically, the spectra display a strong absorption at approximately 267–274 nm and a less intense absorption at 389–393 nm, indicating that the substituents have only a small electronic influence (Figure 3). The fluorescence spectra are characterised by relatively broad, plateau-like emissions from 552 to 572 nm.

Quantum chemical calculations were performed to identify the origins of the transitions in the visible spectral range utilising the range-corrected functional CAM-B3LYP together with Ahlrichs-pvdz douple-ζ basis set and Grimmes dispersion correction (for technical details, see the Supporting Information), which were shown to yield reliable geometries and UV/Vis absorption spectra at reasonable computational cost.[23–28] A comparison between theoretical and experimental spectra is shown in Figure 4 for **16e** as a representative derivative. The theoretical spectra are represented by a stick spectrum that is additionally broadened by simple Gaussians, with a full-width at half-maximum of 0.2 eV and redshifted by 0.8 eV. Results for those derivatives not shown are almost identical; thus, theory reproduces the experimental observation that exchanging the substituent R has little or no influence on the main chromo-

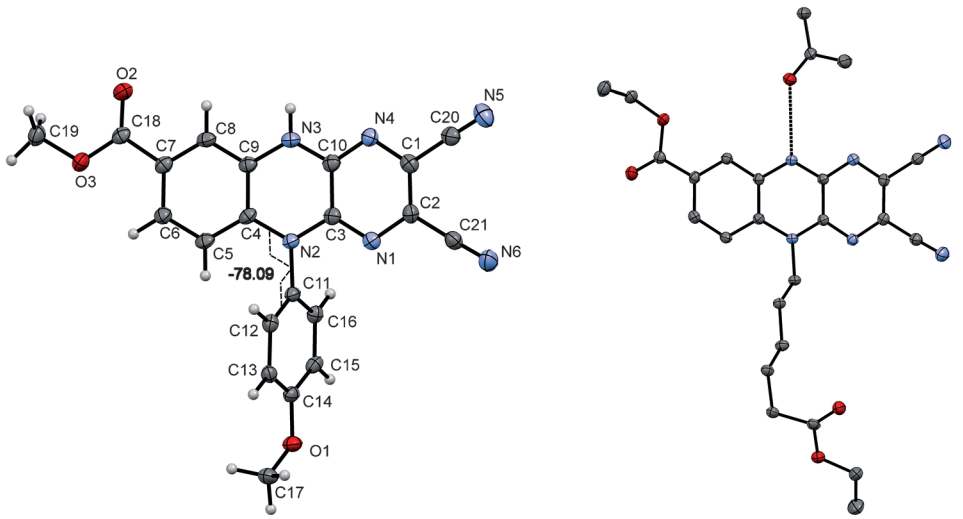

Figure 1. View of **16h** (left) and **16d** (right, H-atoms are omitted for clarity).[35]

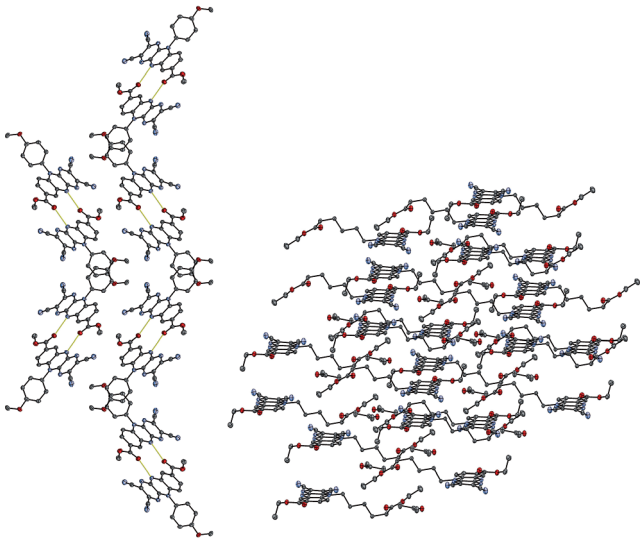

Figure 2. View of molecular packing **16h** (left) and **16d** (right).

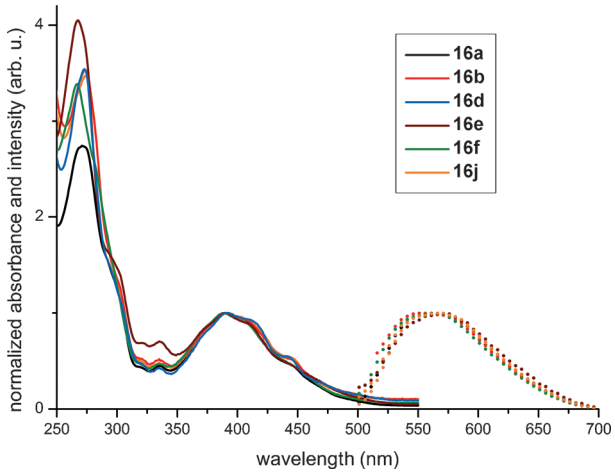

Figure 3. Normalised absorption (line) and emission (points) spectra of selected derivatives **16** in acetonitrile. λ_{max} absorption/emission for **16a**: 389/562 nm; **16b**: 389/552 nm, **16d**: 391/567 nm, **16e**: 391/572 nm, **16f**: 389/565 nm, and **16j**: 388/552 nm.

phore. This is further substantiated by inspection of the optimised ground-state geometries, which were always characterised by a nearly perpendicular arrangement of the phenyl groups R with respect to the main chromophore, thus, decoupling the two (not shown).

The experimental absorption maximum at approximately 400 nm, which shows a vibrational progression, as well as the low-energy shoulder at approximately 500 nm are well reproduced by the TD-DFT calculations. The intense absorption at approximately 400 nm is largely dominated by a π–π^* transition from the HOMO to the LUMO+1 (contribution to the total electronic transition: C_I^2 *100=87.6; the threshold for plotting transition arrows in figures is set at C_I^2 *100=20; arrow thicknesses in the transition schemes scale linearly with C_I^2), whereas the low-energy transition at approximately 500 nm is from HOMO to LUMO. Both transitions show a weak

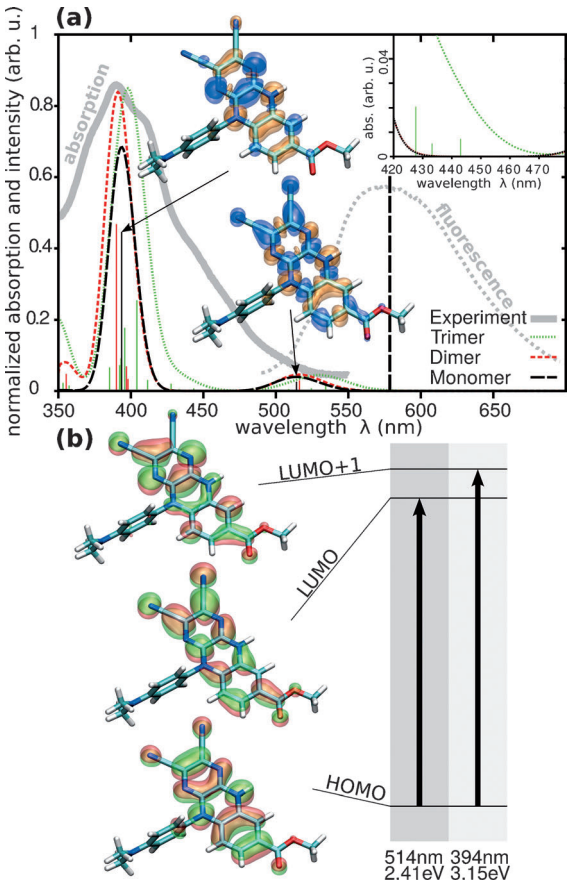

Figure 4. a) Broadened and shifted theoretical (monomer, dimer, trimer: dashed lines) and experimental (solid lines) UV/Vis absorption and fluorescence (right spectra, vertical dashed line in case of theory) spectra of derivative **16e**. Charge difference densities are shown for the most prominent monomer transitions. b) Scheme illustrating the orbital contributions to the energetically lowest two transitions of the monomer compound.

charge transfer towards the cyano substituents in addition to their π–π^* character, as shown by the charge difference densities and canonical molecular orbitals in Figure 4a and b. It is notable that none of the substances **16** show any contribution around 450 nm, where the experimental spectrum exhibits a weak and broad shoulder, in their monomer form according to theory. However, progressing to higher aggregates, weak signals emerge in that spectral region, as shown in the inset in Figure 4a. Hence, theory supports the attribution of features around 450 nm to aggregate effects. As examples, the aggregate spectra of **16a**, **16e** and **16f** were calculated and are shown in the Supporting Information.

Dihydrotetraazatetracenes: Influence of an extended π-system

We investigated the influence of an extended π-system or an additional ester group at the chromophoric system on the spectroscopic properties. The UV/Vis and fluorescence spectra of the three comparable compounds are depicted in Figure 5. As assumed, there is no significant difference between the absorption spectra of the tetraaza-substituted dihydroanthra-

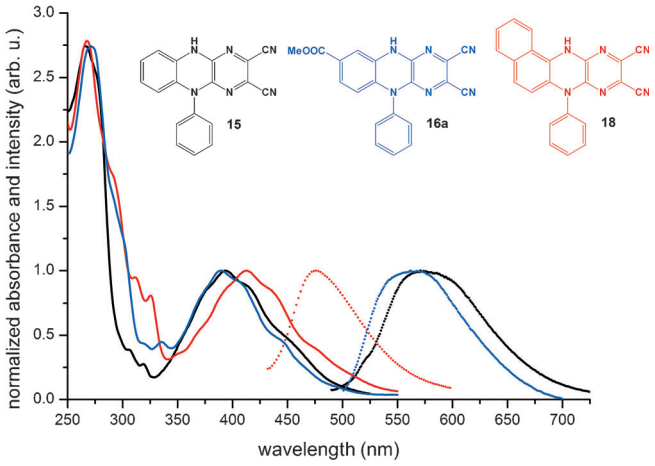

Figure 5. Comparison of the spectral data between the tetraaza-substituted dihydroanthracenes **15**, **16a** and dihydrotetracene **18** in acetonitrile (absorption = line; emission = points). λ_{max} absorption/emission for **15**: 393/571 nm, **16a**: 389/562 nm, and **18**: 413/476 nm.

cenes of type **15**/**16a** and the dihydrotetracene derivative **18**. The enlarged π-system in **18**, compared with those in **15** and **16a**, means that all frontier molecular orbitals are spatially extended (Figure 6). Thus, the LUMO energy of **18** decreases slightly, whereas the energies of HOMO and LUMO + 1 are increased slightly compared with those in **15**. As a consequence, the absorption bands are slightly shifted bathochromically, as seen in the experimental absorption spectra. Furthermore, the energy gap between the first two excited states increases due to the extension of the π-system from **15** to **18**.

In contrast to the rather small spectral differences between the absorption spectra of **15**, **16a** and **18**, a relatively strong deviance was observed in their fluorescence spectra. The tricyclic derivatives exhibit a large shift between the absorption maxima at approximately 390 nm and the fluorescence maxima of approximately 180 nm. However, the onset of the fluorescence spectra fit approximately to the low-energy absorptions at approximately 500 nm (Figure 6). If the low-energy transition is the origin of the fluorescence, the reorganisation energy would be expected to be rather small (energy of vertical transition to the lowest excited state is approximated as 2.49 eV; the 0–0 fluorescence transition energy is estimated at 2.25 eV; thus, the excited state reorganisation energy is approximately 240 meV). The energy difference between the TD-DFT-optimised S^1 state and the S^0 state at the same geometry of an isolated molecule **15** of 2.17 eV (572 nm) approximately match the energy of the experimental fluorescence spectrum (ca. 2.18 eV, ca. 570 nm).

In contrast to the tricyclic derivatives, the fluorescence of the tetracyclic analogue **18** reveals a much smaller shift between the absorption maximum at 413 nm and the fluorescence maximum at 476 nm of only 63 nm. Thus, the fluorescence appears to originate from the major π–π* excited state at 413 nm, even if our TD-DFT calculations again predict a low-energy absorption at 575 nm, but with very low intensity, and a fluorescence at 641 nm. We assume that the transition from the S^2 state to the low-energy S^1 state is either forbidden or occurs at a very low rate in **18**. A more detailed analysis of how the structural modifications from substance **15** to **18** change the excited state dynamics will be carried out in a subsequent work.

The aggregation behaviour of such polycyclic aromatic compounds is crucial for the electronic properties in the solid state or thin film. Therefore, we studied the intermolecular interactions by X-ray single-crystal analysis (see Figure 7). The crystals were grown by slowly evaporating the solvents from solutions of chloroform/ethanol (**15**) or acetonitrile (**18**).

Whereas **15** exhibits dimeric structures, **18** forms a step-like π-stacking network. The distance between those steps is an even 3.315 Å because of an effective interaction, and the polymeric stacks of **18** are connected to each other because of the solvent molecules. Every dihydrotetracene unit is linked by H-bonds to an acetonitrile molecule, which itself interacts with the neighbouring dihydrotetracene stack.

The dimeric structure in the case of **15** results in alternating distances between the planes in the packing; depending on the kind of interaction, they are 3.398 or 3.634 Å. The dimers are connected through H-bonds between the phenyl moieties and the nitrogen of the pyrazine unit from the neighbouring dihydroanthracene plane (3.634 Å). The substructure on the rear of each dimer is related through π-interactions to the next (3.398 Å).

Nitro-substituted dihydrotetraazaanthracenes 17

Compared with derivatives of type **16**, nitro-substituted dihydrotetraazaanthracenes **17** give rise to complex absorption spectra. The strongest absorptions of **17a**–**d** are located at $\lambda =$ 367–376 nm. Whereas alkyl-substituted derivatives **17c** and **17d** show a further absorption at $\lambda \approx 448$ nm, those possessing aromatic residues show only a shoulder. All derivatives in the long-wavelength region exhibit two overlapping peaks between 504 and 550 nm. In the presence of a strong *para*-donor substituent (dimethylamino, **17e**), the spectrum differs from those discussed previously, particularly in the spectral range between 350 and 457 nm, where it features a single broad absorption band that is centred at approximately 430 nm. The absorption bands of derivatives **17a**–**d** between 350 and 457 nm appear to be slightly redshifted in the case of **17f**. In contrast to the other derivatives **17**, lower energetic absorption bands (cf. 475–600 nm) are unresolved for **17f**. Given that all derivatives **17** contain a nitro group, mesomerism is possible, in which the substituted nitrogen acts as an electron donor. This results in a quinoid substructure, in which the nitro group accepts the electron pair (see Scheme 5). Such a structure may be the reason for the strong bathochromically shifted absorbance compared with the other dihydroazaanthracenes described (**15** and **16**).

To enable a reliable interpretation of the peaks found in the absorption spectra of **17** (Figure 8), we performed line-fit analyses of the experimental spectra to deconvolute the electronic transitions from vibrational progression and we performed quantum chemical calculations to unravel the origin of the

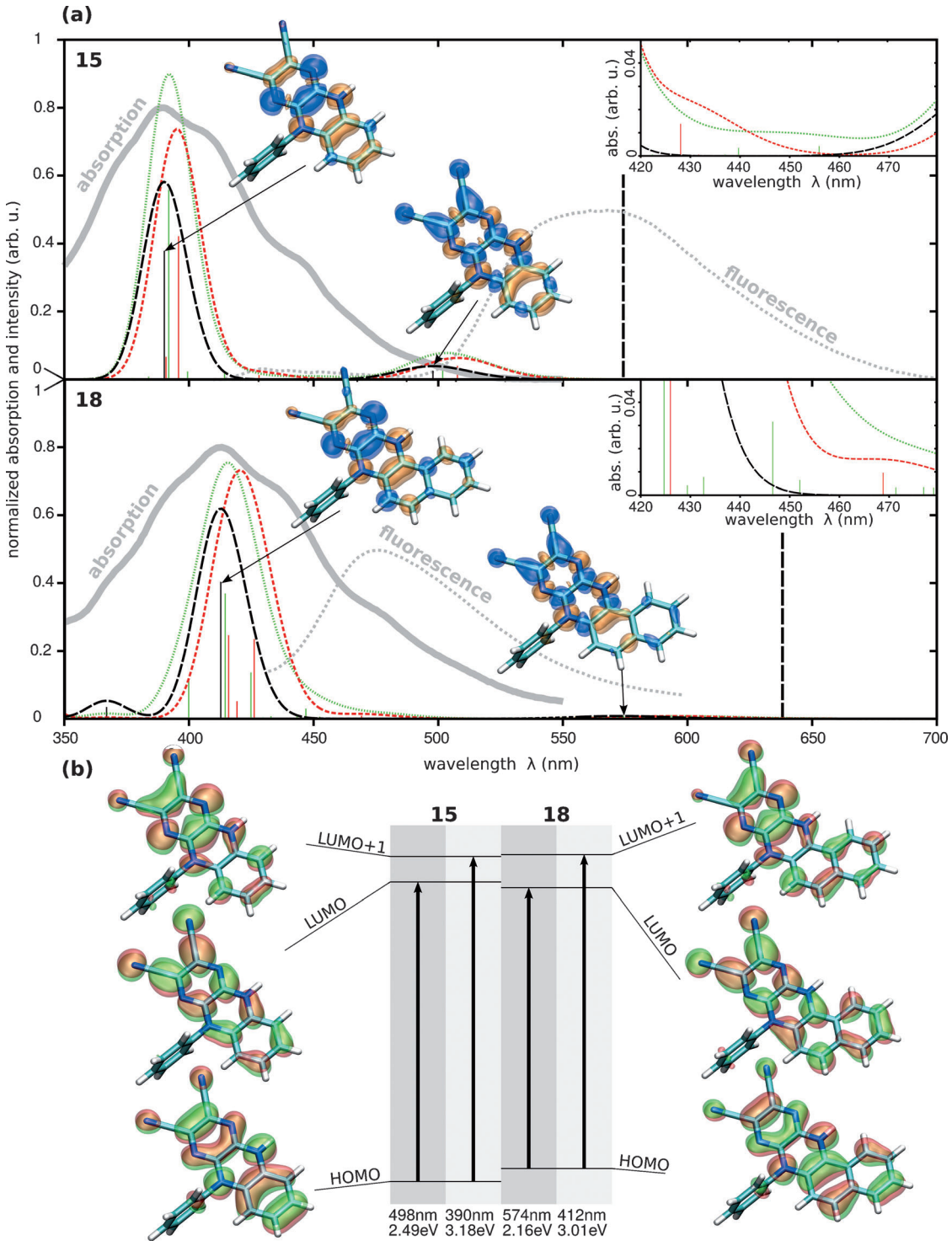

Figure 6. a) Broadened and shifted theoretical (monomer, dimer, trimer: dashed lines) and experimental (solid lines) UV/Vis absorption and fluorescence (right spectra, vertical dashed line in case of theory) spectra of derivatives **15** and **18**. Charge different densities that result instantaneously with photoexcitation are shown for the most prominent monomer transitions. b) Scheme illustrating the orbital contributions to the energetically lowest two transitions of **15** and **18**.

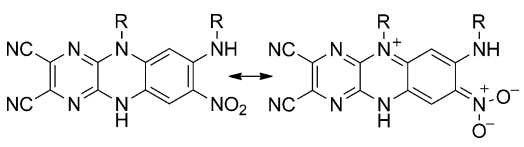

Scheme 5. Mesomeric structures of derivatives **17**.

electronic transitions. As examples, the results of these calculations are shown in Figure 9 for derivatives **17b**, **17d** and **17e**. In contrast to the spectra shown in Figure 4 and Figure 6, we found three prominent peak structures around 525, 425 and 360 nm in Figure 9 to be best described by each using an ordinary vibrational progression[29] (for details see the Supporting

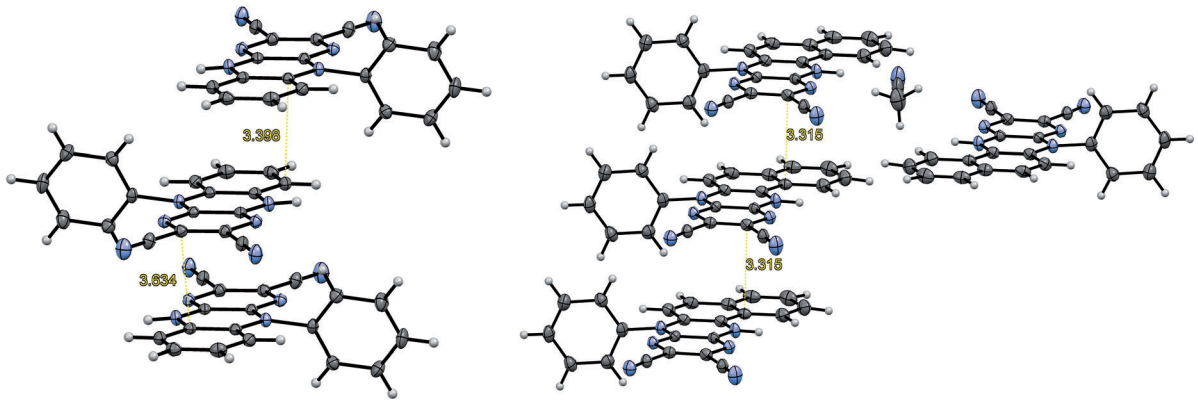

Figure 7. Comparison between the packing of **15** (left) and **18** (right). Yellow lines show the interaction between atoms.[35]

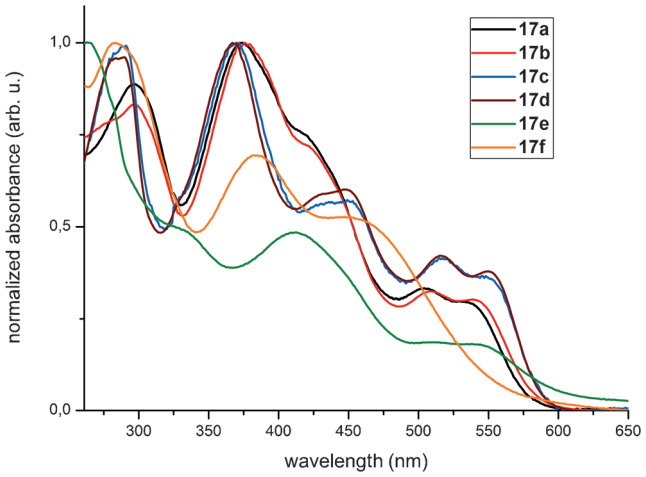

Figure 8. Normalised UV/Vis spectra of selected nitro-substituted dihydrotetraazaanthracenes of type **17** in acetonitrile. λ_{max} absorption for **17a**: 372 nm, **17b**: 376 nm, **17c**: 370 nm, **17d**: 367 nm, **17e**: 413 nm, and **17f**: 382 nm.

Information). The vibrational progressions derived from the experimental spectra are applied to broaden the vertical pure electronic transitions derived from the TD-DFT calculations, as seen in Figure 9. In the TD-DFT calculations, we considered different conformers by means of a generalised rotamer search algorithm[30,31] with subsequent quantum chemical optimisation. We found the central absorptions between 350 and 500 nm of the conformers of any particular derivative **17** to differ significantly only if R contained a phenyl-ring, yielding two distinct conformers in each case: the two residuals pointing away from each other, that is, angular, and a face-to-face configuration of the rings. Alkyl chains turned out to have only a very weak impact on the resulting spectra, although the actual conformer geometries differed greatly.

Considering that the experimental absorption spectra of **17a** and **17b** are very similar (cf. Figure 8), we focus on the spectral features of our TD-DFT results regarding **17b** in the following. As shown in Figure 9, the experimental spectrum could be reproduced well by using a semiempirical approach; that is, by using absorption parameters derived ab initio together with those obtained from line-fits of the experimental spectra, particularly for the face-to-face conformer. The absorption features observed experimentally at 375, 425 and 525 nm originate basically from HOMO to LUMO+2, LUMO+1 and LUMO (in the latter case, the HOMO–LUMO excitation largely dominates the total electronic transition: C_i^2 *100=85) transitions, respectively. Whereas for the face-to-face conformer, only the peak at approximately 525 nm is underestimated in its relative oscillator strength by the TD-DFT calculations, both the peaks at 525 and 425 nm are underestimated for the angular conformer. In the case of the alkyl-substituted derivatives **17c** and **17d**, the experimental absorption spectra are very similar and we focus discussion of the particular features on **17d**. As in the case of **17b**, the simulated absorption spectrum of the **17d** face-to-face conformer (in the case of alkyl-substitution labelled as cisoidal), fits the experimental spectrum better than the simulated absorption spectrum of the angular conformer, as shown in Figure 9. The energy spacing between the three major electronic transitions is particularly large and the long-wavelength absorption at approximately 525 nm is significantly more intense in the case of the cisoidal conformer compared with the angular conformer.

In the case of the dimethyl-amino-phenylene-substituted derivative **17e**, the broad absorption at approximately 430 nm is reproduced basically by a single electronic transition for the angular conformer and by two superposed, similarly intense transitions for the face-to-face conformer. The low-energy absorption between 500 and 550 nm is again predicted to be too low for both conformers, whereas the face-to-face conformer shows significantly higher oscillator strength for this low-energy absorption.

In the case of **17f**, the semiempirical description of the absorption spectra presented above failed because of the lack of visible vibrational progression in the spectra. Furthermore, the theoretical spectra of **17f** could not reproduce the experimental findings at all and, instead, gave results that were qualitatively similar to those obtained with **17e**. This might be due to aggregation effects mediated by the spatially small residuals in the solution and will be subject to further investigation. It should be noted that, given the results shown in Figures 4 and

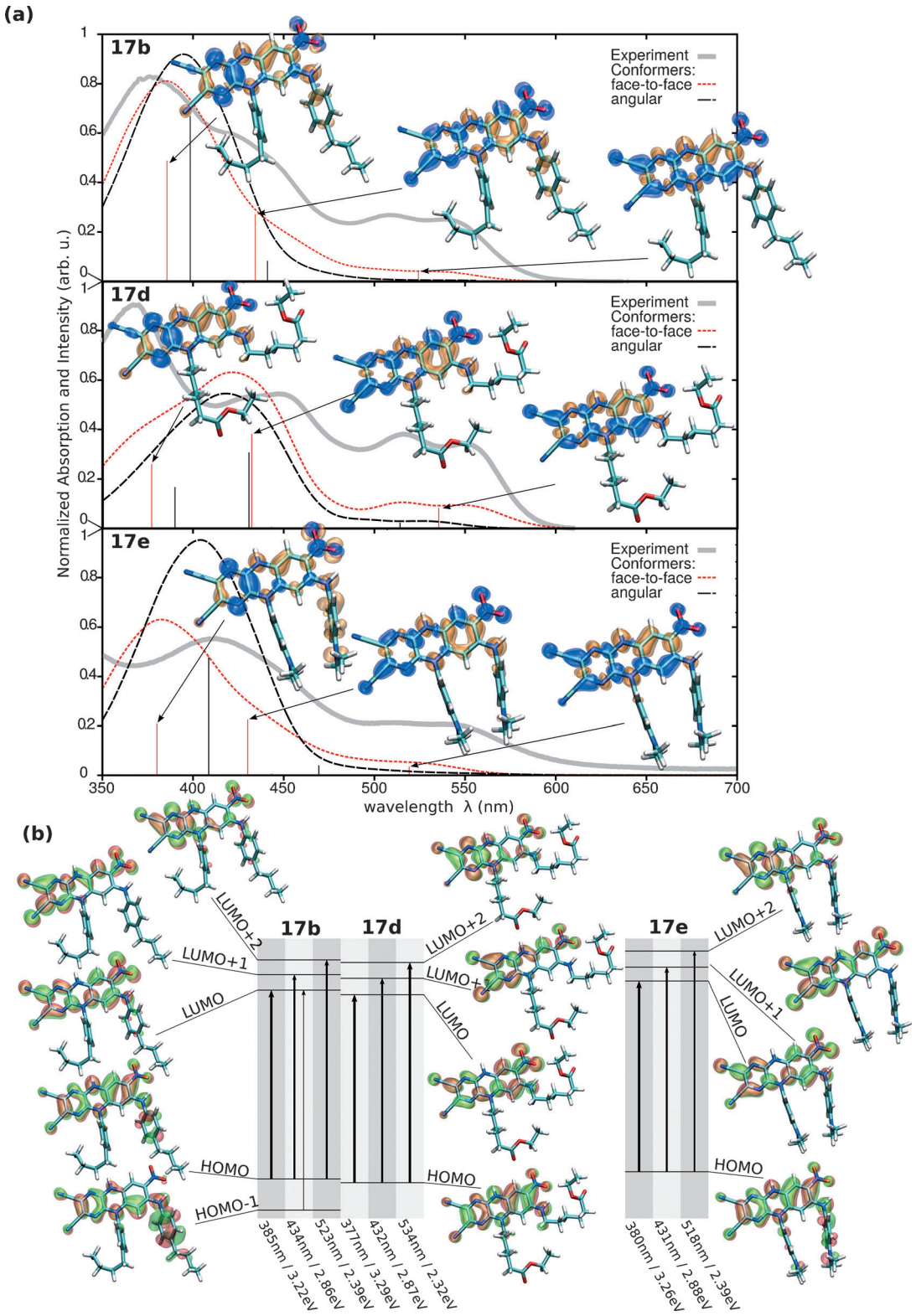

Figure 9. a) Broadened and shifted theoretical (monomer, dashed line) and experimental (solid line) UV/Vis absorption spectra of derivatives **17b**, **17d** and **17e**. Transition densities are shown for the most prominent monomer. b) Scheme illustrating the orbital contributions to the lowest three transitions of the three substances.

6, agreement between theory and experiment is expected to improve if aggregates of derivates **17** are investigated.

Contrary to other dihydrotetraazaanthracenes presented here, none of the nitro derivatives **17** measured showed fluorescence. The changes in the absorption and emission behaviour compared with derivatives **15**, **16** and **18** can possibly be attributed to the presence of the nitro group. This functional

group is well-known for its ability to act as a quencher of fluorescence in many cases.[32]

Imidazodihydroanthracenes

In a first attempt to cyclise the tetramines **11** synthesised in situ with **14**, the yellow-fluorescent imidazodihydroanthracene derivatives **19** were isolated instead of the desired octaazapentacenes (Scheme 6). Most likely, the reason for the formation of

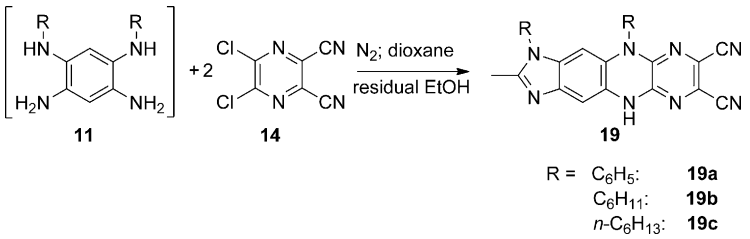

Scheme 6. Tetracyclic imidazoles **19** as unexpected cyclisation products (30–58 %).

derivatives **19** is the oxidising capacity of the cyclisation partner **14**. Together with small amounts of ethanol, which was used as a solvent, acetic acid could be formed in the course of a redox reaction. In a subsequent cyclisation reaction, this reactive acid was able to easily transform one diamine part of **11** to yield the 2-methylimidazole derivatives of type **19**.

These novel imidazole derivatives **19** were isolated in the form of intense yellow-orange solids. Their solubilities increase, as expected, from the phenyl derivative **19a** through **19b** (cyclohexyl) to the long-chained **19c** (*n*-hexyl). The UV/Vis spectra reveal that the chemical nature of the R group does not exert any influence on the chromophoric system (Figure 10). All derivatives show a strong absorption band at 305 nm and a second broad band in the range around 410 nm. Larger differences arise from the fluorescence spectra: whereas derivative **19a** shows a substantial emission at $\lambda = 529$ nm, that of **19c** is bathochromically shifted by 32 nm.

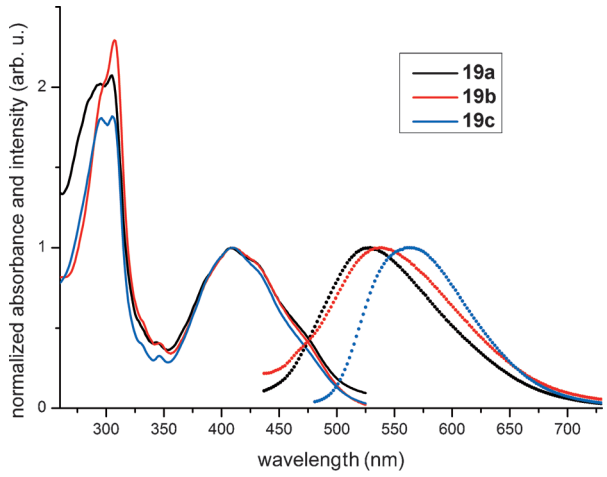

Figure 10. Normalised absorption (line) and emission (points) spectra of compounds **19** in acetonitrile. λ_{max} absorption/emission for **19a**: 408/529 nm, **19b**: 409/539 nm, and **19c**: 409/561 nm.

The similar absorption behaviour of derivatives **19** could be explained by examining their X-ray structure. We succeeded in obtaining single crystals from **19a** and its X-ray crystal structure is depicted in Figure 11. The central tetranuclear unit is almost ideally planar, but the phenyl residues are twisted significantly, with torsion angles of 57.6° (C2-N1-C13-C14) and 68.2° (C4-N2-C19-C24) out of the plane. As a result of this twisting, there is no interaction between the π-electrons of the imidazodihydroanthracene unit and the phenyl moieties. Therefore, the chromophoric system does not seem to be enlarged (in **19a**) compared with the aliphatic substituted derivatives (**19b**, **19c**), which explains the almost identical absorption behaviour of the three derivatives.

A different approach to yield even larger azaacenes than discussed in the previous section was enabled by our development of derivatives **17**. Thus, we succeeded in synthesising derivatives of octaazapentacene of type **22d**, as illustrated in Scheme 7. We were recently successful in reducing the nitro group

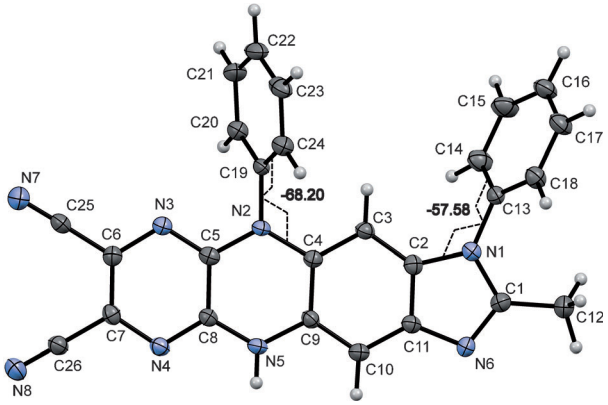

Figure 11. View of **19a** showing the atom-numbering scheme.[35]

in **17d** by means of Pd on activated charcoal and hydrogen gas, and obtained a green fluorescent diamine of type **20d**. This proved to be very sensitive to atmospheric oxygen and was, therefore, cyclised in situ with **14**. In our initial studies, we isolated derivative **22d** in yields of approximately 10 % as a deep-blue solid with gold metallic luster. ^{1}H NMR spectra and MS data indicate the presence of the expected derivative of octaazapentacene. It is noteworthy that the tetrahydro derivative **21d** formed primarily was immediately oxidised to the mesoionic azaacene (Scheme 7). It was nearly impossible to isolate the intermediate substance **21d**; the red solution very rapidly becomes blue with red emission (Scheme 7). Furthermore, we could not detect N–H signals in the ^{1}H NMR spectrum. Additionally, the pentacene obtained shows similar spectroscopic properties to that of the mesoionic hexaazapentacene developed by Fleischhauer et al.,[33] particularly with respect to the broad-structured absorption behaviour in the orange to red region of the visible spectrum. However, the absorption is, perhaps due to the electron-withdrawing cyano residues, slightly redshifted by approximately 21 nm compared

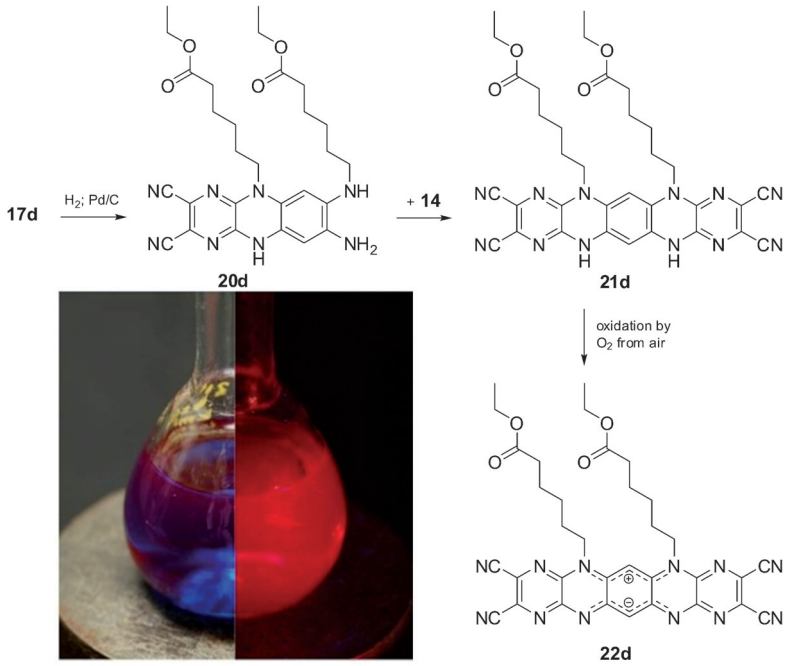

Scheme 7. Using the building block for synthesis of higher azaacenes; for example, derivative **17 d**. Photographs of compound **22 d** dissolved in CH_2Cl_2 in daylight (left) and under irradiation with $\lambda = 365$ nm (right).

with the hexaazapentacene described by Fleischhauer. In addition, the small Stokes shift of the red emission points to low energy loss after excitation, which is typical for rigid systems such as higher acenes.[34] The positions of residues in diamine **20 d** mean that the pentacene has to be mirror symmetric, as depicted in derivative **21 d**. Currently, we cannot provide any information concerning the electronic state; however, experimental data (ESR measurements) suggest a singlet and thus mesoionic state for molecule **22 d**. This is consistent with the findings of other groups for hexaazaanthracenes[14b] and hexaazaacridines.[14c]

To our knowledge, the synthesised pyrazinacene **22 d** represents the zwitterionic pentacene with the highest number of N atoms discovered to date.

Conclusion

Our attempt to develop novel dihydrotetraazaanthracenes **16** and **17** as new materials for use in organic electronic devices has been realised by cyclisation reactions of *N*-substituted *o*-phenylenediamines with **14** in moderate yields. Analogously, 1-amino-2-phenylaminonaphthalene was successfully transformed into dihydrotetraazatetracene **18**. The presence of moieties such as bromine groups or ester substructures means that derivatives **16** provide opportunities to introduce further functional groups through cross-coupling or transesterification reactions. All new derivatives feature intense absorptions in the yellow-orange region of the visible spectrum. Donor/acceptor substituents at the peripheric phenyl moieties affect, in the case of derivatives **16**, their UV/Vis spectra only slightly. Whereas dihydrotetraazaanthracenes **16** and dihydrotetraazatetracene **18** show dramatically different shifted fluorescence, hence indicating slow relaxation from higher excited states to the S^1 state in **18**, none of the nitro derivatives of type **17** are fluorescent. An unexpected result was obtained by cyclisation of tetramines **10**, synthesised in situ, with **14**. Instead of tetrahydrooctaazapentacenes **21**, the yellow-fluorescent derivatives of imidazodihydroanthracenes **19** were isolated and fully characterised. All three groups of dihydrotetraazaacenes presented here possess the preconditions to serve as building-blocks for higher azaacenes (see Scheme 8). The nitro group of derivates **17** can be reduced to another vicinal diamine, which, in subsequent reactions, can be cyclised with a wide range of bis-electrophilic partners (e.g., with **14** to the mesoionic octaazapentacenes **22**). Additionally, all our dihydroazaacenes contain a vicinal dicyano substructure, which is suitable for further condensation reactions with diamines. Previously, this twofold extrusion of hydrogen cyanide formed the basis for the synthesis of a series of edge-sharing condensed oligopyrazine analogues.[8] By using both routes, we were already successful in the synthesis of higher azaacenes, which are redox switchable systems with interesting properties such as high photostability, large molar extinction coefficient and fluorescent quantum yield. We will report in a forthcoming paper on the use of derivatives **17** as starting material for the construction of derivatives of octaazapentacene and their redox behaviour, as well as on other unsymmetrical azaacenes, using **16**, and their application as functional dyes.

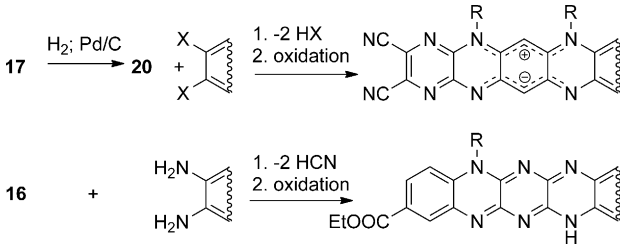

Scheme 8. Dihydroazaanthracenes as suitable building blocks for higher azaacenes.

Experimental Section

Further details of the synthetic procedures, quantum chemical calculations, NMR spectra and single-crystal X-ray data can be found in the Supporting Information.

Acknowledgements

We thank Professor Todd Martínez and Julia Preiß for scientific exchange and support. Additionally, we thank Dr. Günther, G. Sentis and H. Heinecke from HKI Jena for measuring the NMR spectra, Mrs Schönau and Mrs Heineck for the measurement of the MS spectra. M.K., T.S. and M.P. gratefully acknowledge financial support from the "Bundesministerium für Bildung und Forschung" (FKZ: 03K3507). T.S. furthermore acknowledge financial support from the "Deutsche Bundesstiftung Umwelt".

Keywords: chromophores · cyclization · density functional calculations · nitrogen heterocycles · sensitizers

[1] a) M. A. Green, K. Emery, Y. Hishikawa, W. Warta, E. D. Dunlop, *Prog. Photovoltaics* **2014**, *22*, 1 – 9; b) J. You, L. Dou, K. Yoshimura, T. Kato, K. Ohya, T. Moriarty, K. Emery, C.-C. Chen, J. Gao, G. Li, Y. Yang, *Nat. Commun.* **2013**, *4*, 1446 – 1456; c) R. Fitzner, E. Mena-Osteritz, A. Mishra, G. Schulz, E. Reinold, M. Weil, C. Korner, H. Ziehlke, C. Elschner, K. Leo, M. Riede, M. Pfeiffer, C. Uhrich, P. Bäuerle, *J. Am. Chem. Soc.* **2012**, *134*, 11064 – 11067.

[2] a) M. Grätzel, *J. Photochem. Photobiol. C* **2003**, *4*, 145 – 153; b) P. Wang, S. M. Zakeeruddin, J. E. Moser, M. K. Nazeeruddin, T. Sekiguchi, M. Grätzel, *Nat. Mater.* **2003**, *2*, 402 – 407; c) M. Grätzel, *Acc. Chem. Res.* **2009**, *42*, 1788 – 1798; d) S. Tschierlei, M. Presselt, C. Kuhnt, A. Yartsev, T. Pascher, V. Sundström, M. Karnahl, M. Schwalbe, B. Schäfer, S. Rau, M. Schmitt, B. Dietzek, J. Popp, *Chem. Eur. J.* **2009**, *15*, 7678 – 7688; e) B. Schäfer, H. Görls, M. Presselt, M. Schmitt, J. Popp, W. Henry, J. G. Vos, S. Rau, *Dalton Trans.* **2006**, *18*, 2225 – 2231.

[3] a) N. Li, D. Baran, K. Forberich, F. Machui, T. Ameri, M. Turbiez, M. Carrasco-Orozco, M. Drees, A. Facchetti, F. C. Krebs, C. J. Brabec, *Energy Environ. Sci.* **2013**, *6*, 3407 – 3413; b) M. Grätzel, R. A. J. Janssen, D. B. Mitzi, E. H. Sargent, *Nature* **2012**, *488*, 304 – 312; c) H. Hoppe, N. S. Sariciftci, *J. Mater. Res.* **2004**, *19*, 1924 – 1945; d) M. Al-Ibrahim, H. K. Roth, U. Zhokhavets, G. Gobsch, S. Sensfuss, *Sol. Energy Mater. Sol. Cells* **2005**, *85*, 277; e) F. C. Krebs, *Sol. Energy Mater. Sol. Cells* **2009**, *93*, 465 – 475; f) L. Blankenburg, K. Schultheis, H. Schache, S. Sensfuss, M. Schroedner, *Sol. Energy Mater. Sol. Cells* **2009**, *93*, 476 – 483.

[4] F. C. Krebs, *Org. Electron.* **2009**, *10*, 761 – 768.

[5] a) A. R. Reddy, M. Bendikov, *Chem. Commun.* **2006**, 1179 – 1181; b) O. Berg, E. L. Chronister, T. Yamashita, G. W. Scott, R. M. Sweet, J. Calabrese, *J. Phys. Chem. A* **1999**, *103*, 2451 – 2459; c) J. E. Anthony, *Angew. Chem. Int. Ed.* **2008**, *47*, 452 – 483; *Angew. Chem.* **2008**, *120*, 460 – 492; d) L. B. Roberson, J. Kowalik, L. M. Tolbert, C. Kloc, R. Zeis, X. Chi, R. Fleming, C. Wilkins, *J. Am. Chem. Soc.* **2005**, *127*, 3069 – 3075; e) O. D. Jurchescu, M. Popinciuc, B. J. vanWees, T. T. M. Palstra, *Adv. Mater.* **2007**, *19*, 688 – 692; f) O. D. Jurchescu, J. Baas, T. T. M. Palstra, *Appl. Phys. Lett.* **2004**, *84*, 3061 – 3063; g) T. Minakata, Y. Natsume, *Synth. Met.* **2005**, *153*, 1 – 5; h) J. Takeya, C. Goldmann, S. Haas, K. P. Pernstich, B. Ketterer, B. Batlogg, *J. Appl. Phys.* **2003**, *94*, 5800 – 5804.

[6] a) P. J. S. Foot, V. Montgomery, C. J. Rhodes, P. Spearman, *Mol. Cryst. Liquid Cryst.* **1993**, *236*, 199 – 204; b) H.-Y. Chen, I. Chao, *ChemPhysChem* **2006**, *7*, 2003 – 2007; c) J. I. Wu, C. S. Wannere, Y. Mo, P. v. R. Schleyer, U. H. F. Bunz, *J. Org. Chem.* **2009**, *74*, 4343 – 4349; d) Y.-Y. Liu, C.-L. Song, W.-J. Zeng, K.-G. Zhou, Z.-F. Shi, C.-B. Ma, F. Yang, H.-L. Zhang, X. Gong, *J. Am. Chem. Soc.* **2010**, *132*, 16349 – 16351.

[7] a) S. Miao, A. L. Appleton, N. Berger, S. Barlow, S. R. Marder, K. I. Hardcastle, U. H. F. Bunz, *Chem. Eur. J.* **2009**, *15*, 4990 – 4993; b) U. H. F. Bunz, *Pure Appl. Chem.* **2010**, *82*, 953 – 968; c) G. J. Richards, J. P. Hill, T. Mori, K. Ariga, *Org. Biomol. Chem.* **2011**, *9*, 5005 – 5017; d) Q. Miao, *Synlett* **2012**, *23*, 326 – 336; e) U. H. F. Bunz, J. U. Engelhart, B. D. Lindner, M. Schaffroth, *Angew. Chem. Int. Ed.* **2013**, *52*, 3810 – 3821; *Angew. Chem.* **2013**, *125*, 3898 – 3910.

[8] G. J. Richards, J. P. Hill, N. K. Subbaiyan, F. D'Souza, P. A. Karr, M. R. J. Elsegood, S. J. Teat, T. Mori, K. Ariga, *J. Org. Chem.* **2009**, *74*, 8914 – 8923.

[9] a) C. Seillan, H. Brisset, O. Siri, *Org. Lett.* **2008**, *10*, 4013 – 4016; b) Z. He, D. Liu, R. Mao, Q. Tang, Q. Miao, *Org. Lett.* **2012**, *14*, 1050 – 1053.

[10] a) F. Stöckner, R. Beckert, D. Gleich, E. Birckner, W. Günther, H. Görls, G. Vaughan, *Eur. J. Org. Chem.* **2007**, 1237 – 1243; b) Z. He, R. Mao, D. Liu, Q. Miao, *Org. Lett.* **2012**, *14*, 4190 – 4193; c) J. U. Engelhart, B. D. Lindner, O. Tverskoy, F. Rominger, U. H. F. Bunz, *Org. Lett.* **2012**, *14*, 1008 – 1011.

[11] G. J. Richards, J. P. Hill, K. Okamoto, A. Shundo, M. Akada, M. R. J. Elsegood, T. Mori, K. Ariga, *Langmuir* **2009**, *25*, 8408 – 8413.

[12] a) Y. Fogel, M. Kastler, Z. Wang, D. Andrienko, G. J. Bodwell, K. Müllen, *J. Am. Chem. Soc.* **2007**, *129*, 11743 – 11749; b) S. Miao, S. M. Brombosz, P. v. R. Schleyer, J. I. Wu, S. Barlow, S. R. Marder, K. I. Hardcastle, U. H. F. Bunz, *J. Am. Chem. Soc.* **2008**, *130*, 7339 – 7344.

[13] F. Wudl, P. A. Koutentis, A. Weitz, B. Ma, T. Strassner, K. N. Houk, S. I. Khan, *Pure Appl. Chem.* **1999**, *71*, 295 – 302.

[14] a) J. Preßler, R. Beckert, S. Rau, R. Menzel, E. Birckner, W. Günther, H. Görls, *Z. Naturforsch.Sect. B* **2012**, *67*, 0367 – 0372; b) K. Hutchison, G. Srdanov, R. Hicks, H. Yu, F. Wudl, *J. Am. Chem. Soc.* **1998**, *120*, 2989 – 2990; c) P. Langer, A. Bodtke, N. N. R. Saleh, H. Görls, P. R. Schreiner, *Angew. Chem. Int. Ed.* **2005**, *44*, 5255 – 5259; *Angew. Chem.* **2005**, *117*, 5389 – 5393.

[15] G. T. W. Ried, *Liebigs Ann. Chem.* **1988**, 1197 – 1199.

[16] J. Nishida, N. Naraso, S. Murai, E. Fujiwara, H. Tada, M. Tomura, Y. Yamashita, *Org. Lett.* **2004**, *6*, 2007 – 2010.

[17] R. M. Z. He, R. Mao, D. Liu, Q. Miao, *Org. Lett.* **2012**, *14*, 4190 – 4193.

[18] a) E. Clar, *The Aromatic Sextet*, Wiley, New York, **1972**; b) Q. Miao, T. Q. Nguyen, T. Someya, G. B. Blanchet, C. Nuckolls, *J. Am. Chem. Soc.* **2003**, *125*, 10284 – 10287.

[19] a) K. Shang, J. Gallagher, N. M. Bie, F. Li, Q. Che, Y. Wang, Y. Jiang, *J. Org. Chem.* **2014**, *79*, 5134 – 5144; b) S. Munack, V. Leroux, K. Roderer, M. Ökvist, A. van Eerde, L.-L. Gundersen, U. Krengel, P. Kast, *Chem. Biodiversity* **2012**, *9*, 2507 – 2527.

[20] H. G. O. Becker, *Organikum*, 23rd ed., Wiley-VCH, Weinheim, **2009**.

[21] A. J. Boydston, C. S. Pecinovsky, S. T. Chao, C. W. Bielawski, *J. Am. Chem. Soc.* **2007**, *129*, 14550 – 14551.

[22] a) E. E. Kostyuchenko, V. F. Traven, R. A. Mkhitarov, B. I. Stepanov, *Zh. Org. Khim.* **1980**, *16*, 1702 – 1707; b) L. F. Tietze, Th. Eicher, Reaktionen und Synthesen im organisch-chemischen Praktikum und Forschungslaboratorium, 2nd ed., Thieme, Stuttgart, **1991**, 324.

[23] T. Yanai, D. P. Tew, N. C. Handy, *Chem. Phys. Lett.* **2004**, *393*, 51 – 57.

[24] A. Schäfer, H. Horn, R. Ahlrichs, *J. Chem. Phys.* **1992**, *97*, 2571 – 2576.

[25] S. Grimme, J. Antony, S. Ehrlich, H. Krieg, *J. Chem. Phys.* **2010**, *132*, 154104.

[26] S. Grimme, S. Ehrlich, L. Goerigk, *J. Comput. Chem.* **2011**, *32*, 1456 – 1465.

[27] W. J. D. Beenken, F. Herrmann, M. Presselt, H. Hoppe, S. Shokhovets, G. Gobsch, E. Runge, *Phys. Chem. Chem. Phys.* **2013**, *15*, 16494 – 16502.

[28] W. Beenken, M. Presselt, T. H. Ngo, W. Dehaen, W. Maes, M. Kruk, *J. Phys. Chem. A* **2014**, *118*, 862 – 871.

[29] S. T. Hoffmann, H. Bässler, A. Köhler, *J. Phys. Chem. B* **2010**, *114*, 17037 – 17048.

[30] N. M. O'Boyle, M. Banck, C. A. James, C. Morley, T. Vandermeersch, G. R. Hutchison, *J. Cheminf.* **2011**, *3*, 1 – 33.

[31] The Open Babel Package, version 2.3.0, http://openbabel.org, accessed February, **2014**.

[32] S. Shanmugaraju, S. A. Joshi, P. S. Mukherjee, *J. Mater. Chem.* **2011**, *21*, 9130 – 9138.

[33] J. Fleischhauer, S. Zahn, R. Beckert, U.-W. Grummt, E. Birckner, H. Görls, *Chem. Eur. J.* **2012**, *18*, 4549 – 4557.

[34] A. L. Appleton, S. Barlow, S. R. Marder, K. I. Hardcastle, U. H. F. Bunz, *Synlett* **2011**, *14*, 1983 – 1986.

[35] CCDC-1032655 (**15**), 1032659 (**16d**), 1032658 (**16h**), 1032660 (**18**) and 1032657 (**19b**) contain the supplementary crystallographic data for this paper. These data can be obtained free of charge from The Cambridge Crystallographic Data Centre via www.ccdc.cam.ac.uk/data_request/cif..

Received: January 19, 2015
Published online on ■■ ▮▮, 0000

FULL PAPER

Sensitizers

D. M. Gampe, M. Kaufmann, D. Jakobi, T. Sachse, M. Presselt, R. Beckert, H. Görls*

■■ – ■■

Stable and Easily Accessible Functional Dyes: Dihydrotetraazaanthracenes as Versatile Precursors for Higher Acenes

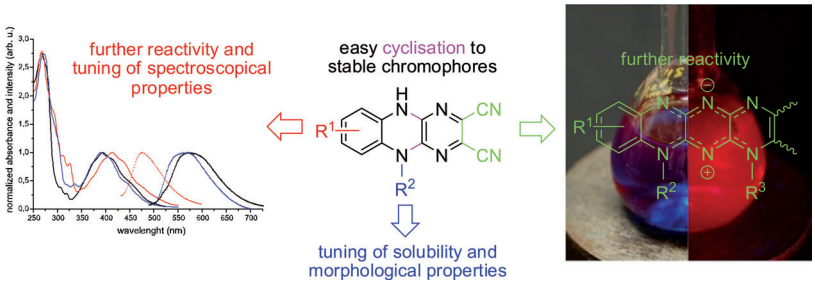

Dihydroazaacenes: A series of dihydrotetraazaanthracenes and one new dihydrotetraazatetracene as substances for applications in organoelectronic devices and as suitable building blocks for higher azaacenes was synthesised. Single-crystal X-ray analyses were carried out to examine the morphology and solid packing effects. Finally, a dihydrotetraazaanthracene was used as a building-block to create a mesoionic octaazapentacene.